MODELING AND TORQUE PULSATION REDUCTION FOR A SWITCHED RELUCTANCE MOTOR DRIVE SYSTEM

[**]Bin-Yen Ma, [*]Tian-Hua Liu, and [**]Wu-Shiung Feng

[*]Department of Electrical Engineering
National Taiwan Institute of Technology
Taipei, Taiwan 106, R. O. C.

[**]Department of Electrical Engineering
National Taiwan University
Taipei, Taiwan 106, R. O. C.

ABSTRACT

This paper presents a new method for analysis and design of a three-phase switched reluctance drive system. First, the mathematical models of a switched reluctance motor under an a-b-c stationary frame and a d-q synchronous frame are proposed. Next, two current command waveforms that produce a lower torque pulsation than traditional switched reluctance drives are discussed. Finally, some simulation and experimental results are presented to validate the theoretical analysis. This paper presents a new direction in analysis and control of a switched reluctance motor.

I. INTRODUCTION

Switched reluctance drive technology has undergone significant development over the last two decades. Compared with the induction drive or the permanent magnet synchronous drive, the switched reluctance drive has many advantages, for example, the simple and rugged construction of the motor. It has high efficiency and can endure high temperatures because its rotor has no winding. The switched reluctance drive system, therefore, can be operated efficiently in hostile environments. There have been many studies on the switched reluctance drive. For example, Miller et. al developed a drive system for a switched reluctance motor [1]. Lipo. et. al proposed a new salient reluctance motor drive [2]. In addition, M. Ehsani et. al studied sensing rotor position by measuring mutually induced voltages or a frequency modulated converter [3]. However, these papers studied the switched reluctance

---

motor by using only the a-b-c stationary frame. In addition, the phase current command of the drive system is a square waveform due to the assumption that each phase's self-inductance of the motor is a trapezoidal waveform. In the real world, however, the self-inductance is not a trapezoidal waveform because of the nonlinear nature of the switched reluctance motor. Torque pulsation is therefore produced.

In this paper, first the models of a three-phase switched reluctance motor (SRM) under an a-b-c stationary frame and a d-q synchronous frame are presented. The torque equation is derived according to the real self-inductances of the SRM. Next, two improved current command waveforms of the SRM are derived. These current commands produce lower torque pulsation. Finally, some simulated and experimental results validate the theoretical analysis. This paper proposes a new direction in the study of the SRM.

II. SYSTEM DESCRIPTION AND MODELING

A. System Description

The block diagram of a switched reluctance drive system is shown in Fig. 1. This system consists of four major parts: a motor, a current-regulated converter, a controller, and sensors. First, the controller computes the speed error and then executes the control algorithm. Next, the controller determines and outputs the current commands to the current-regulated converter. The current-regulated converter controls the three phase currents to follow the current commands. The sensors consist of the current and position sensors. The whole system consists of a current loop and a speed loop. By suitably adjusting the amplitude and frequency of the currents, a closed-loop system is thus achieved.
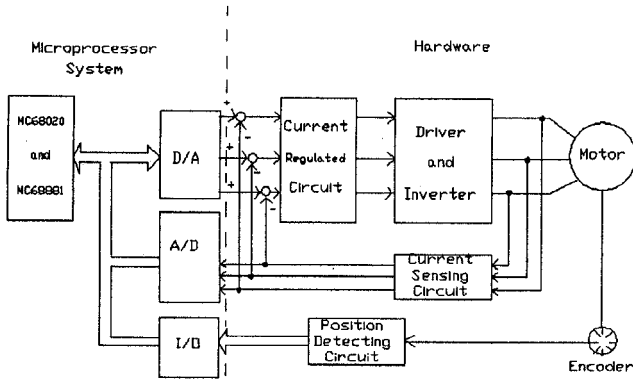
Fig. 1 Block diagram of a SRM drive system.

The SRM consists of two parts: stator and rotor. The stator has concentrated windings but the rotor has no winding. Both stator and rotor are salient structures. The air gap, therefore, is not uniform.

B. Stationary frame model

The SRM is a nonlinear system. Generally speaking, the self–inductance of the motor is related to the position of the rotor. We can assume that each phase's self–inductance is not related to its phase current or the other phase's self–inductance because their correlation is very small. The flux linkage of the motor, therefore, can be expressed as

$$\lambda_j(\theta_e, i_j) = L_j(\theta_e)\, i_j \qquad\qquad j=a, b, c \qquad (1)$$

where λ_j is the flux linkage of each (a, b, c) phase, L_j is each phase's self–inductance, i_j is each phase's current, and θ_e is the electrical rotating angle. The self–inductance of different phases has the same shape but shifts a 120° electrical phase angle. The dynamic equation of each phase voltage is

$$v_j(\theta_e) = R_s\, i_j + \frac{d}{dt}\lambda_j\,(\theta_e, i_j)$$

$$= R_s\, i_j + L_j(\theta_e)\frac{d}{dt} i_j + i_j \frac{dL_j(\theta_e)}{d\theta_e}\omega_r \qquad (2)$$

where v_j is the phase voltage, R_s is the phase resistance, and ω_r is the electrical rotating speed. The torque of the motor is

$$T_e(\theta_e, i_j) = N_r \sum_{j=a,b,c} \frac{\partial}{\partial\theta_e}\int_0^{i_j} L_j(\theta_e)\, i_j\, di_j$$

$$= N_r\, (\frac{1}{2} i_a^2 \frac{dL_a(\theta_e)}{d\theta_e} + \frac{1}{2} i_b^2 \frac{dL_b(\theta_e)}{d\theta_e} + \frac{1}{2} i_c^2 \frac{dL_c(\theta_e)}{d\theta_e}) \quad (3)$$

where N_r is the number of rotor teeth, L_a, L_b, and L_c are the a, b, c phases' self–inductances. The electrical speed of the motor is

$$\frac{d}{dt}\omega_r \frac{1}{N_r} = \frac{1}{J_m}(T_e - B_m\omega_r \frac{1}{N_r} - T_l) \qquad (4)$$

where J_m is the inertia, B_m is the viscous coefficient, and T_l is the external load.

C. Synchronous frame model

The relationship transformation between d–q axis and a–b–c axis can be expressed as

$$\begin{bmatrix} f_q \\ f_d \\ f_0 \end{bmatrix} = \begin{bmatrix} \cos\theta_e & \cos(\theta_e-120^\circ) & \cos(\theta_e+120^\circ) \\ \sin\theta_e & \sin(\theta_e-120^\circ) & \sin(\theta_e+120^\circ) \\ 0.5 & 0.5 & 0.5 \end{bmatrix}\begin{bmatrix} f_a \\ f_b \\ f_c \end{bmatrix}$$

$$= T(\theta)\, f_{abc} \qquad (5)$$

where f_q is the synchronous q–axis voltage or current, f_d is the synchronous d–axis voltage or current, f_0 is the zero–sequence voltage or current, T is the a–b–c to d–q axis transformation, and f_a, f_b, f_c are the stationary a, b, c–axis voltages or currents. The synchronous d–q axis voltage equations are

$$v_q = R_s\, i_q + \omega_r\, \lambda_d + p\, \lambda_q \qquad (6)$$

$$v_d = R_s\, i_d - \omega_r\, \lambda_q + p\, \lambda_d \qquad (7)$$

where v_q is the q–axis voltage, i_q is the q–axis current, ω_r is the electrical speed, λ_d is the d–axis flux, p is the differential operator, λ_q is the q–axis flux, v_d is the d–axis voltage, and i_d is the d–axis current. The torque of the motor is

$$T_e = \frac{3}{2} N_r\, (\lambda_d\, i_q - \lambda_q\, i_d) \qquad (8)$$

III. TORQUE PULSATION REDUCTION

The major disadvantage of the SRM is that its torque pulsation is larger than other machines. There are many papers which have proposed different methods to reduce the torque pulsation of a SRM. These papers [4]–[5],

however, have not presented simple and systematic methods to derive the phase current command waveforms which can reduce torque pulsation. This motivated us to study this subject. Fig. 2 shows the ideal self–inductance waveforms and the ideal current command waveforms of a SRM. Each self–inductance increases/decreases linearly when its related stator and rotor teeth move closer or farther away. The self–inductance is maintained at a constant when its related stator and rotor teeth are aligned. According to the self–inductance waveforms, we can obtain the ideal phase current commands which can produce maximum average torque and minimum torque pulsations. The current command of each phase is a square wave with a 1/3 duty cycle. Each phase's current is injected into the motor when its related self–inductance is increased. By summing–up the three–phase torque, we can obtain the smoothing torque. In a real system, the self–inductance, however, is not a trapezoidal waveform. The real self–inductance can be approximately expressed as [3], [4]:

$$L_a(\theta_e)=L_{ls}+L_A-L_{B1}\cos(\theta_e)+\sum_{n=2,3...}^{N} L_{Bn}\cos(n\theta_e) \quad (9)$$

$$L_b(\theta_e)=L_{ls}+L_A-L_{B1}\cos(\theta_e-120^\circ)$$
$$+\sum_{n=2,3..}^{N} L_{Bn}\cos[n(\theta_e-120^\circ)] \quad (10)$$

$$L_c(\theta_e)=L_{ls}+L_A-L_{B1}\cos(\theta_e+120^\circ)$$
$$+\sum_{n=2,3..}^{N} L_{Cn}\cos[n(\theta_e+120^\circ)] \quad (11)$$

and

$$\theta_e=N_r\theta_{rm} \quad (12)$$

where L_{ls} is the leakage inductance, L_A, L_{B1}, L_{Bn} are the parameters of the self–inductance, and θ_{rm} is the mechanical shaft angle.

Inductances (ideal)
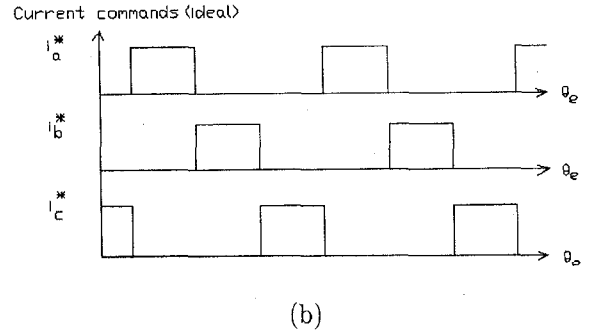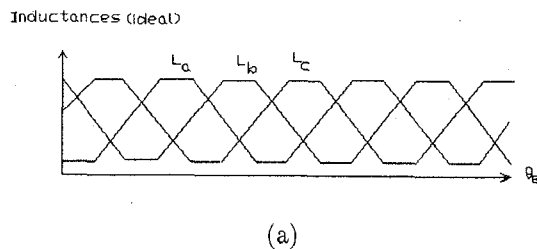
(a)

Current commands (ideal)

(b)

Fig. 2 Waveforms of the SRM (a) ideal inductances (b) ideal current commands.

The self–inductances are not trapezoidal waveforms. In this paper, some modified current command waveforms, have therefore been derived according to the proposed a–b–c and d–q coordinate mathematical models.

A. METHOD 1

Method 1 is derived from the stationary frame model of the motor. Take the a–phase as an example: the torque produced by the a–phase is

$$T_a = T_e= \text{constant} \qquad \theta_{a\ on}\leq \theta_e \leq \theta_{a\ off}$$
$$=0 \qquad\qquad \text{else} \qquad (13)$$

The electrical conduction period of the a–phase is

$$\theta_{a\ cond}= \theta_{a\ off} - \theta_{a\ on}$$
$$= \frac{360}{q} \quad (14)$$

where $\theta_{a\ cond}$ is the electrical conduction period of the a–phase current command, $\theta_{a\ off}$ is the electrical turn–off angle of the a–phase current, $\theta_{a\ on}$ is the electrical turn–on angle of the a–phase current, and q is the phase number of the motor. From equations (3), (9), and (13), we can obtain

$$i_a(\theta_e)=\frac{\sqrt{T_a}}{\sqrt{0.5N_r(L_{B1}\sin\theta_e+ \sum_{n=2,3...}^{N} L_{Bn}\ n\ \sin(n\theta_e))}} \quad (15)$$

The b–phase and c–phase current commands show the same waveforms as the a–phase, however, the b–phase lags/leads the a–phase 120° and the c–phase lags/leads the a–phase 240° when the motor is in clockwise/counter clockwise rotation.

B. Method 2

In method 2, first we select only the fundamental and dc components as the self–inductance. The harmonics of the self–inductance in equations (9)–(11) are neglected because they are very small when compared with the fundamental component [6]. Then, the approximate inductances are

$$L_a'(\theta) \cong L_{ls} + L_A - L_{B1}\cos(\theta_e) \qquad (16)$$

$$L_b'(\theta) \cong L_{ls} + L_A - L_{B1}\cos(\theta_e - 120^\circ) \qquad (17)$$

$$L_c'(\theta) \cong L_{ls} + L_A - L_{B1}\cos(\theta_e + 120^\circ) \qquad (18)$$

where L_a', L_b', L_c' are approximate values of the self–inductances in the a–b–c stationary frame. The approximate values of the self–inductances in the d–q synchronous frame are:

$$\begin{bmatrix} L_q' & 0 & 0 \\ 0 & L_d' & 0 \\ 0 & 0 & L_0' \end{bmatrix} = T(\theta)^{-1} \begin{bmatrix} L_a'(\theta_e) & 0 & 0 \\ 0 & L_b'(\theta_e) & 0 \\ 0 & 0 & L_c'(\theta_e) \end{bmatrix} T(\theta)$$

$$= \begin{bmatrix} L_{ls}+L_A-L_{B1} & 0 & 0 \\ 0 & L_{ls}+L_A+L_{B1} & 0 \\ 0 & 0 & L_{ls} \end{bmatrix} \qquad (19)$$

where L_d' and L_q' are the approximate values of the d–q axis inductances. The L_d' and L_q' are constant values. If the current commands are sinusoidal waveforms, the mutual inductances have to be considered. Then, the L_d' and L_q' of the equation (19) are multiplied by 1.5. The d–q axis currents (i_d and i_q), which are orthogonal, can be defined as

$$i_d = i_s \cos\delta \qquad (20)$$

$$i_q = i_s \sin\delta \qquad (21)$$

and

$$i_s = \sqrt{i_d^2 + i_q^2} \qquad (22)$$

$$\delta = \tan^{-1}(i_q / i_d) \qquad (23)$$

where i_s is the amplitude of the current vector, δ is the phase angle of the current vector. The torque can be

derived from equation (8), and it is expressed as

$$T_e = \frac{3}{2} N_r (L_d' - L_q') i_d i_q \qquad (24)$$

If we choose $\delta = 45^\circ$, then the torque ratio T_e/i_s has a maximum value, and this control is called "maximum torque" control. On the other hand, if we maintain i_d as a constant, and only adjust i_q, then the torque is proportional to i_q. This is called "field oriented" control. The phase currents i_a, i_b, i_c can be computed according to the coordinate transformation:

$$\begin{bmatrix} i_a \\ i_b \\ i_c \end{bmatrix} = T(\theta) \begin{bmatrix} i_q \\ i_d \\ i_0 \end{bmatrix} \qquad (25)$$

The current command waveforms i_a, i_b, i_c are sinusoidal waveforms in spite of maximum torque or field oriented controls. By suitably adjusting the amplitude, frequency, and phase, the torque can be effectively controlled. The torque pulsation due to the harmonics of the self–inductances is neglected here. The reason is that the harmonics of each phase self–inductance are much smaller when compared with the fundamental sinusoidal component of the self–inductance. If we consider both the average torque and the torque pulsation, then

$$T_e = \frac{3}{2} N_r (2L_{B1}) i_d i_q + \frac{3}{2} N_r \sum_{n=2,3...}^{N} (2nL_{Bn}) i_{dn} i_{qn} \quad (26)$$

where i_{dn} and i_{qn} are the equivalent d–q axis currents with the shaft angle $n\theta_e$. The currents i_{dn} and i_{qn} have the shaft rotating speed $n\omega_e$ because they are related to the nth harmonics of the self–inductances.

IV. SIMULATION AND EXPERIMENTAL RESULTS

The implemented system is shown in Fig. 1. The SRM is 3 phase, 8 pole (rotor), 10 HP. The parameters of each phase of the self–inductance are L_{ls} = 7.5mH, L_A = 90mH, L_{B1} = 32.5mH, L_{B2} = −4.9mH, L_{B3} = 0.622mH, L_{B4} = 2.2mH, L_{B5} = −1.52mH. The other parameters of the SRM are: R_s = 2Ω, J_m = 0.0222N–m–sec^2/rad, and

$B_m = 0.00028$ N–m–sec/rad. A unipolar current regulated converter is designed for the traditional square wave current command and the proposed method 1 current command. Another bipolar current–regulated converter is implemented for the sinusoidal waveforms (method 2). The digital controller is implemented by a 32–bit 16.7MHZ Motorola MC68020 monoboard microprocessor. The controller determines the reference stator currents by looking up tables. The sensors consist of three Hall–effect sensors and an encoder. Some simulated and experimental results are shown here. Fig. 3 shows the simulated torque to rotor shaft position curves (a–phase) for different waveform commands. Method 1 performs better than any other method. Method 2 has the advantage that no phase commutation is required. In the real world, therefore, the torque pulsation due to phase commutation can be eliminated by using method 2. The traditional square wave performs the worst because the self–inductances of the SRM are not trapezoidal waveforms. Fig. 4 shows the measured and simulated current waveforms of the stator. The waveforms are measured from the implemented drive system. The a–phase self–inductance of the SRM is shown in Fig. 5. The inductance is not trapezoidal but close to sinusoidal waveform with harmonics. Fig. 6 shows the torque–current curves of proposed method 2. When kept at the same current amplitude i_s, the maximum torque control produces larger torque than the field oriented control. However, the speed–loop controller design of maximum torque control is more difficult due to its nonlinear relationship between torque and the q–axis current. Fig. 7 shows the measured speed responses of the different current commands.
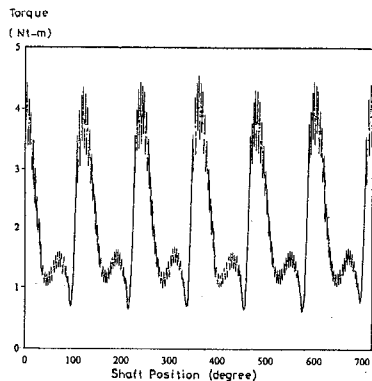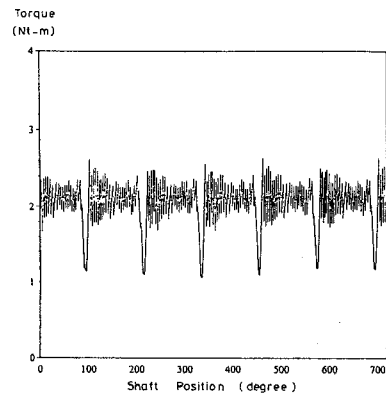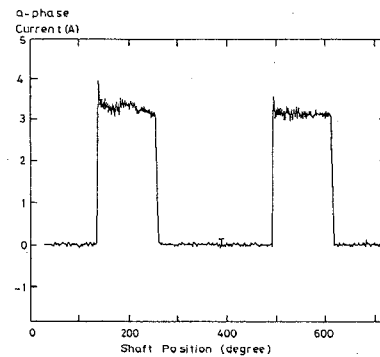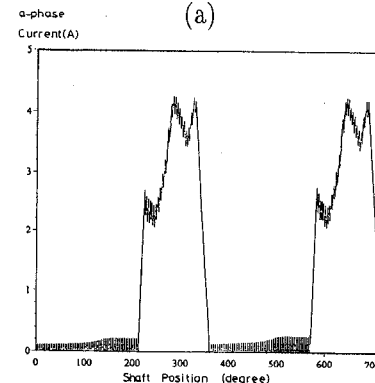

(b)
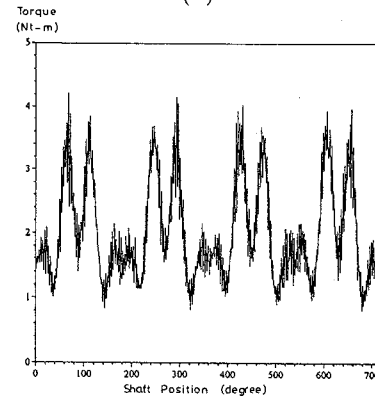
(c)

Fig. 3 Steady–state torque of different current commands (T_l=2N.m)(a)square wave (b)method 1 (c)method 2.

(a)

(b)

(a)
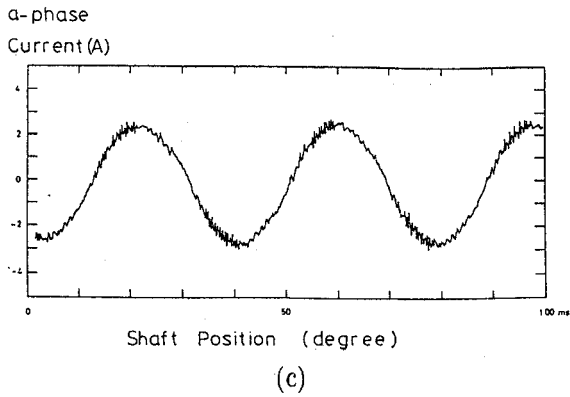
a-phase
Current (A)

Shaft Position (degree)

(c)

Fig. 4 Current waveforms (a)square wave (measured)
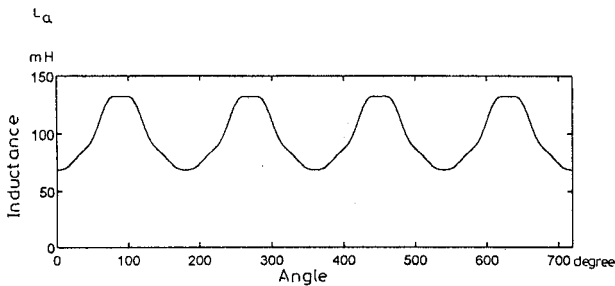(b)method 1 (simulated) (c)method 2 (measured).

L_a

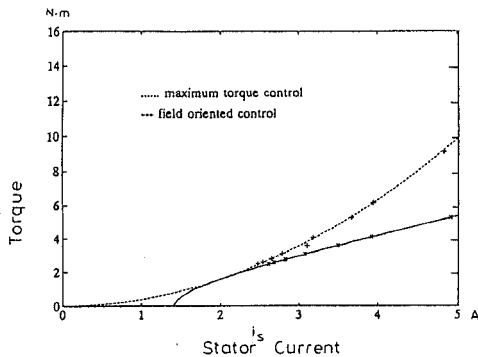Fig. 5 The self–inductance of the SRM (the a–phase).

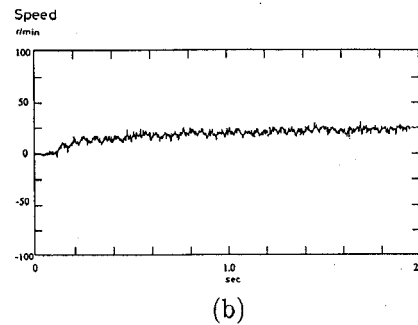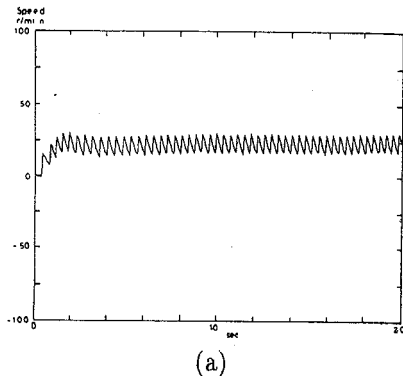Fig. 6 Torque–current curves of method 2.

(a)

Speed
r/min

(b)

Fig. 7 Speed response (a) square wave (b) method 2.

V. CONCLUSIONS

In this paper, three different current waveforms for a SRM are studied. These current waveforms perform with different torque characteristics. The theoretical analysis and experimental results are presented. The experimental results show the possibility of using these proposed command waveforms to replace traditional square wave commands. This paper proposes a new direction in the design of a SRM drive system.

REFERENCES

[1] M. R. Harris, J. W. Finch, J. A. Mallick, and T. J. E. Miller, "A review of the integral–horsepower switched reluctance drive," IEEE Trans. Ind. Appl., vol. IA–22, no. 4, pp. 716–721, July/Aug 1986.

[2] L. Xu, T. A. Lipo, and S. C. Rao, "Analysis of a new variable–speed singly reluctance motor utilizing only two transistor switches," IEEE Trans. Ind. Appl., vol. IA–26, no. 2, pp. 229–236, Mar./Apr. 1990.

[3] I. Husain and M. Ehsani, "Rotor position sensing in switched reluctance motor drives by measuring mutually induced voltages," IEEE Trans. Ind. Appl., vol. IA–30, no. 3, pp. 665–672, May/June 1994.

[4] R. S. Wallace, D. G. Taylor, "A balanced commutator for switched reluctance motors to reduce torque ripple," IEEE Trans. Pow. Electron., vol. PE–7, no. 4, pp. 617–626, Oct. 1992.

[5] D. S. Reay, M. M. Moud, T. C. Green, and B. W. Williams, "Switched reluctance motor control via fuzzy adaptive systems," IEEE Control Systems, vol. 15, no. 3, pp. 8–15, June 1995.

[6] N. Matsui, N. Akao, and T. Wakino, "High precision torque control of reluctance motors," IEEE Trans. Ind. Appl., vol. IA–27, no. 5, pp. 902–907, Sep./Oct. 1991.